Africa Journal of Physical Sciences Vol. 5, pp. 63-79, December 2020
http://journals.uonbi.ac.ke/index.php/ajps/index
ISSN 2313-3317

Artificial Neural Network for Prediction of Pollution Load of Lead, Copper, and Cadmium in a Water Resource: A case Study of River Sosiani, Eldoret Municipality, Kenya

OBIEWA James Oduor[1a*], KARIUKI David Kinuthia[1b], and WACHIRA-MBUI Damaris Nduta[1c]

[1]Department of Chemistry, University of Nairobi, Nairobi, P.O. Box 30197 – 00100, Kenya
[a*]jamesobiewa@gmail.com, [b] kkariuki@uonbi.ac.ke, [c]dmbui@uonbi.ac.ke

ARTICLE INFO

Article History:
Submitted: 14 October 2020
Accepted: 31 December 2020
Available online: December 2020

Keywords:
Artificial neural network
Correlation Pollution load
Water resource

ABSTRACT

This study aimed at predicting the pollution load of Lead, Copper, and Cadmium in river Sosiani using the Artificial Neural Network, based on parameters, Physico-chemical; turbidity, Electrical Conductivity, and Chemical Oxygen Demand, and Chemical; fluoride and phosphate. The Atomic Absorption Spectrophotometer, Ultra Violet-Visible Spectrophotometer, Ion Selective electrodes and Redox-titration methods were used for analysis in from six sample sites, S1 to S6. A total of 78 datasets from the experimental results were used and divided into three, training 60%, testing 20%, and holdout 20%. The model used the IBM SPSS statistics 20 software, and performances evaluated using Pearson's correlation coefficient. The mean pollution loads from laboratory analysis were 0.615±0.293, 0.037±0.027, and 0.096±0.030 mg/L while those from ANN were 0.615±0.293, 0.032±0.023, and 0.073±0.033 mg/L for Pb, Cu, and Cd, respectively. The correlation coefficients between the ANN and the observed values for Pb, Cu, and Cd were 0.9999, 0.9910, and 0.9965, respectively. The ANN was able to predict the pollution load of Pb, Cu, and Cd in the river.

ISSN 2313-3317

1. Introduction

Pollutants emanating from industries often deposit in water resources such as rivers, lakes, and oceans. Pollution impacts of a water resource depend on the pollution quantity and assimilative capacity of the water body [1, 2]. Many water quality parameters have been implicated to potentially affect the availability of metal cations in a water resource. For example, specific adsorption, precipitation, and complexation greatly affect the distribution of the metal ions in a water body. An artificial neural network is an interconnected assembly of simple processing units or nodes, whose functionality simulates the animal neuron. The processing ability of an ANN is in the inter-unit connection strengths, or weights, obtained by learning from a set of training patterns [3]. The neurons do not require any prior structural knowledge of the relationships that exist between variables and the processes to be modeled [4]. Approximately 1.8 million children under 5 years die due to waterborne diseases. The trace elements ' concentration in a water resource above WHO recommended limits are a health risk to consumers downstream[2].

The quality of a water resource varies from time to time and therefore, the continuous monitoring of the quality parameters is necessary. Experimental analysis of water quality in laboratories of water resources is time-consuming and expensive. A similar study reported concentrations of lead and cadmium in the Sosiani River that exceeded the WHO standards [2]. It is on this background that this study explores the potential of an artificial neural network to predict concentrations of select pollutants in a water resource using physico-chemical and chemical parameters' assessment. For the assessment of water resources, it is essential to establish an evaluation system of water quality parameters [5]. Long-term exposure to low concentrations of lead, copper, and cadmium can cause many adverse health effects. There are many laboratory analytical methods used to determine trace element concentrations in water resources like atomic absorption spectrometry and Ultraviolet-Visible spectrophotometric methods [6].

In a study carried out in Iran, SO_4, Cl, and TDS were used as input variables to predict the concentrations of some trace elements; Fe, Mn, Pb, and Zn. The findings showed that Multi-output Adaptive Neural Inference System-MANFIS model had the potential to estimate the distribution of the trace elements in groundwater with a high degree of accuracy and robustness [7]. A similar study by [8] used Artificial Neural Network optimized by the Imperialist Competitive Algorithm-ANN-ICA model to predict the concentrations of trace elements in groundwater resources and reported good model performance.
In the prediction of metal cations in Moroccan aquatic sediments, the multi-layer perceptron neuron networks performed better than the multiple linear regressions [9]. A study by [10] used physico-chemical parameters EC, COD, and BOD for the evaluation of wastewater quality. However, this study used the physico-chemical and chemical parameters to predict pollution loads of Pb, Cu, and Cd in the water resource.

The COD, BOD, and TSS were used as input variables in the ANN to predict the performance of the wastewater treatment plant in Alexandria, Egypt, and reported a correlation coefficient of 0.90 between observed and predicted output variables. The artificial neural network in the study proved to be a better tool for simulating, controlling, and predicting the performance of wastewater treatment plants-WWTP [11]. In this study, the pollution load of a surface water resource, river Sosiani that cuts across Eldoret municipality in northern Kenya, was evaluated using Artificial Neural Network. This study used a double-layered ANN model in the prediction of pollution load of Pb, Cu, and Cd in the surface water. The successful application of the ANN in the prediction of pollution loads of a water resource will not only improve rapid assessment but also reduce the cost of water quality monitoring of river Sosiani. The findings of the present study will be of interest to environmentalists, water resources conservationists, water service providers, and policy-makers.

1.1 Artificial neural networks

Artificial intelligence has now come of age, with the current powerful computers and internet connectivity as well as computer programmings culminating into the internet of things-IoT [12]. A given unit or node is a simplified model of a real neuron that sends off a new signal if it receives a sufficiently strong input signal from the other nodes to which it is connected. It trains the algorithm and predicts the error between actual output and simulated output from ANN and propagates backward through the network. During the training process, it reduces the errors between each successive layer and continues until the pre-specified error limits [13]. Among the developed neural network models are

multilayer perceptron, MLP, and radial basis function, RBF, networks [4]. Neural networks differ in their learning processes and architecture. Feed-forward ANN allows signals to travel one way [14].
The artificial neural network training is through supervised learning in which the network is given input and marching output patterns. The ANN learns to perform a particular task by adjusting the values of the connections between elements through a back-propagation algorithm until the network output matches the target variable so that the network can predict the correct targets for a given set of inputs [11]. Figure 1 shows a mathematical model of an artificial neuron.

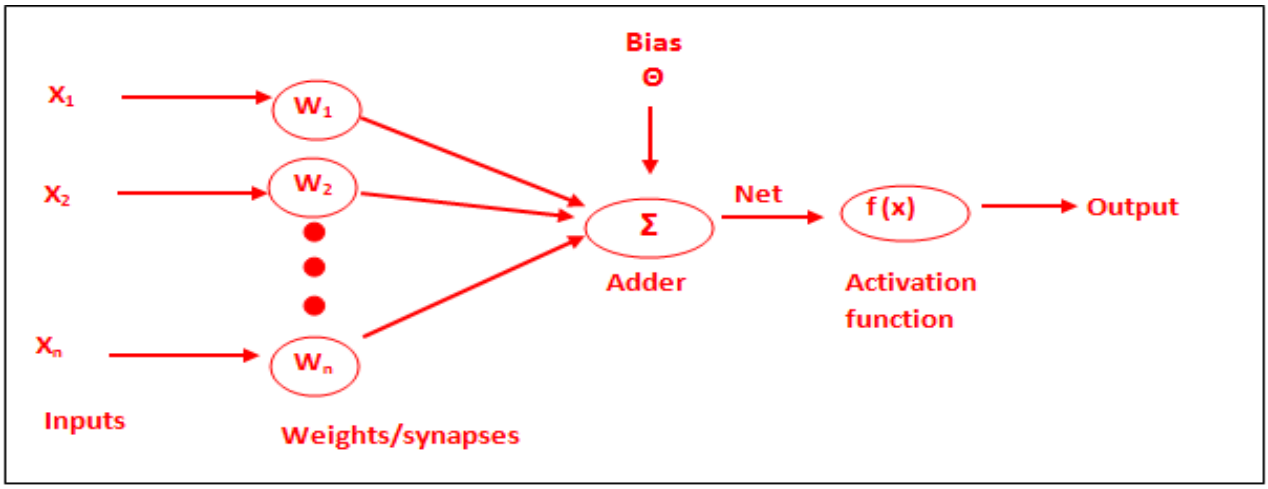

Figure 1: Model of an artificial neuron
Source: [3]

A processing unit which known as neuron, sums the inputs, adds its bias, and then applies a nonlinear transfer function such as hyperbolic tangent or identity function. Finally, an output line transmits the output to other neurons as shown in Figure 1.

1.2 Biological neural networks

The human brain is the most complex structure known, and understanding its operation represents one of the more difficult and exciting challenges faced by science. Biological neural networks provide a driving force behind a great deal of research into artificial network models, which is complementary to the desire to build better pattern recognition and information processing systems. The human brain contains around 10^{11} electrically active cells called neurons. The branching tree of dendrites provides a set of inputs to the neuron, while the axon acts as an output. Communication between neurons takes place at junctions called synapses. Each neuron typically makes connections to many thousands of other neurons so that the total number of synapses in the brain exceeds 10^{14} [15]. Although each neuron is a relatively slow information processing system, the massive parallelism of information processing at many synapses simultaneously leads to a greater processing power, which exceeds that of present-day supercomputers. It also leads to a high degree of fault tolerance, with many neurons dying each day with a little adverse effect on performance [16]. Many neurons act in an all-or-nothing manner, and when they spike, they send an electrical impulse (called an action potential), which propagates from the cell body along the axon. When this signal reaches a synapse, it triggers the release of chemical

neurotransmitters that cross the synaptic junction to the next neuron. Depending on the type of synapse, this can either increase (excitatory synapse) or decrease (inhibitory synapse) the probability of the subsequent neuron firing. Each synapse has an associated strength (or weight), which determines the magnitude of the effect of an impulse on the post-synaptic neuron. Each neuron thereby computes a weighted sum of the inputs from other neurons, and if this stimulation exceeds some threshold, the neuron fires. The fundamental property of both real and artificial neural systems is their ability to modify their responses as a result of exposure to external signals [15,3]. Figure 2 illustrates a biological neural network.

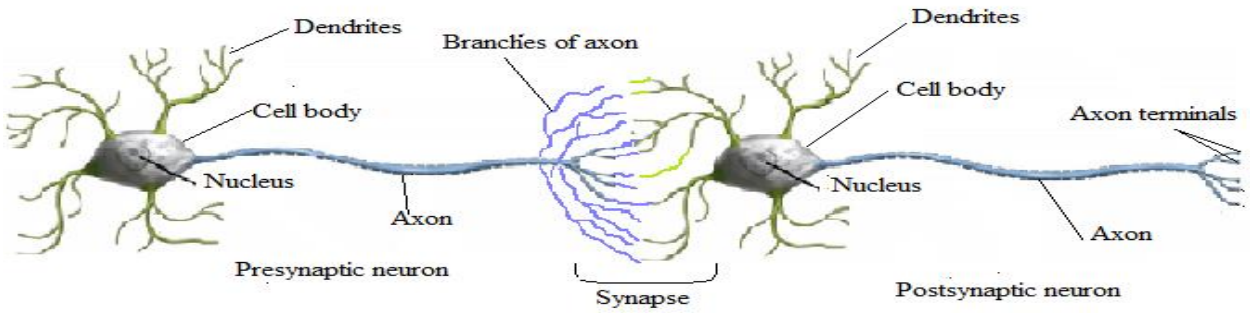

Figure 2: A biological neural network

Source: [17]

Dendrites are fibres that emanate from the cell body and provide the receptive zones that receive activations from other neurons. The cell body (soma) sums the incoming signals. The action potential transmission is along the axon to other neurons or structures outside the nervous systems, e.g., muscles. The junctions that allow signal transmission between the axons and dendrites are called synapses. The transmission process is by diffusion of chemicals called neurotransmitters across the synaptic cleft. In neural networks, information storage is at the synapses [15]. In living organisms, synaptic weights change in response to external stimuli. An unpleasant experience will change the synaptic weights of an organism, which will train to behave differently [17].

1.3 Activation functions

An activation function manipulates the presented data through some gradient processing, usually gradient descent, and afterward produces an output for the neural network that contains the parameters in the data. The activation functions can be either linear or nonlinear based on the functions represented and are used to control the outputs of neural networks. The activation function links the weighted sums of units in a layer to the values of units in the next layer [18].

For a linear model, the input vector x transformation is given by equation 1:

$$f(x) = wx + b \quad (1$$

Where:

x = inputs, w = weights, b = biases

The bias is a scalar parameter that gives the neuron the possibility of shifting the function to the left or right and makes the neuron more powerful. The neural networks produce linear results from the mappings from equation 1, and the need for activation function arises, first to convert these linear outputs to nonlinear output for further computation, especially to learn patterns in data. The outputs of these models are given by equation 2:

$$y = (w_1x_1 + w_2x_2 + \ldots\ldots + w_nx_n + b) \quad (2)$$

These outputs of each layer are relayed to the next subsequent layer for multilayered networks until the final prediction. The expected target outputs determine the type of activation function to use in a given ANN. These activation functions are transfer functions, which are applied to the results of the linear models to produce the transformed non-linear results ready for further processing [18]. The non-linear output after the application of the activation function is given by equation 3:

$$Y = a\,(w_1x_1 + w_2x_2 + \text{-----} + w_nx_n + b) \quad (3)$$

Where *a* is the activation (transfer) function.

Some of the used activation functions include:
The identity activation is used in the output layer when the outputs are real values. It transfers the signals received unchanged, as shown in equation 4.

$$f(x) = x \quad (4)$$

Hyperbolic Tangent function:

The hyperbolic tangent function is one of the activation functions used in deep learning. Tanh is a smoother zero-centred function whose range lies between -1 to 1 and is defined as shown in equation 5:

$$Tanh = \frac{Sinh(x)}{Cosh(x)} = \frac{e^x - e^{-x}}{e^x + e^{-x}} \quad (5)$$

Tanh is used mostly in the hidden layers of multilayer networks. Figure 3 illustrates the hyperbolic tangent function.

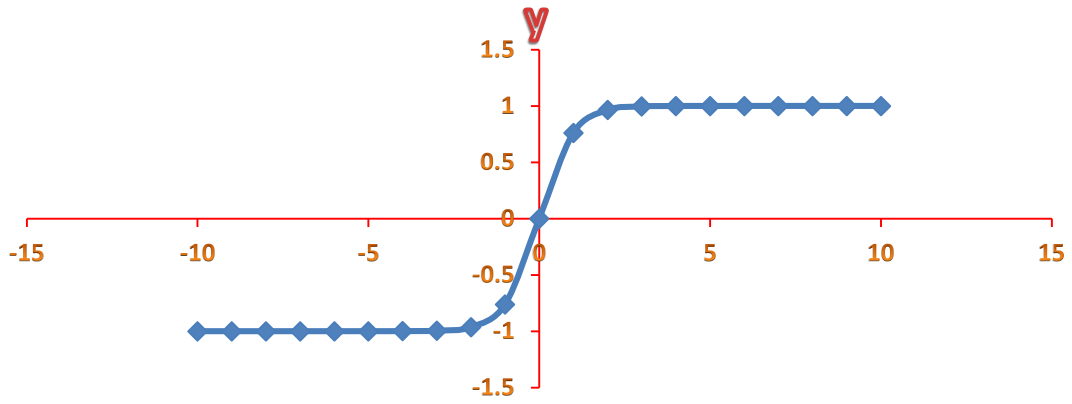

Figure 3: Hyperbolic tangent activation function

2. Materials and Methods

2.1 Study area

The water quality parameters in river Sosiani, in Eldoret municipality, Kenya, were analyzed. The physico-chemical parameters included; turbidity, electrical conductivity, and chemical oxygen demand; chemical parameters fluoride and phosphate; lead, copper, and cadmium. Figure 4 shows a map of the studyarea.

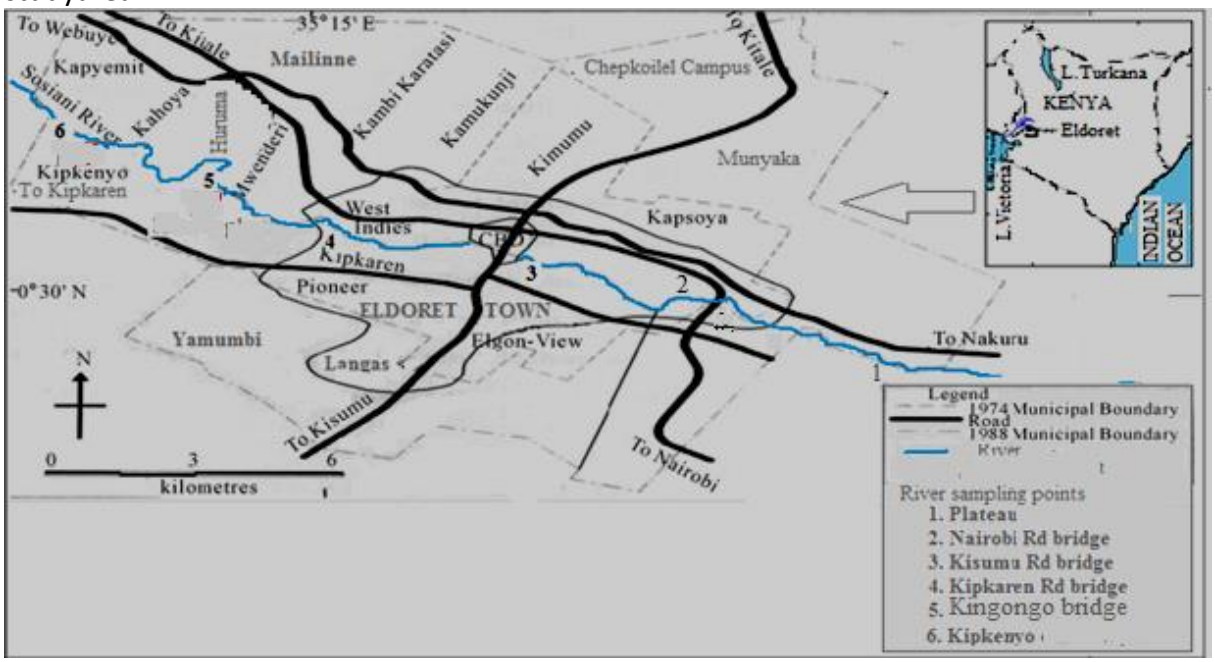

Figure 4: Map showing sampling points along river Sosiani
Source: [2].

2.2 Water sampling and pretreatment

Sampling was carried out twice each during the months of June; July; and August; 2019 at six sampling points on river Sosiani. The water samples were analysed for the physico-chemical parameters turbidity, electrical conductivity, and chemical oxygen demand; chemical parameters fluoride and phosphate; lead, copper, and cadmium. The sample containers were washed twice using the river water before sample collection and sealing. Samples for the Pb, Cu, and Cd analysis were collected in 1-litre plastic bottles, which had been pre-cleaned with 3 % nitric acid and rinsed with deionized water, and then taken to the laboratory for the analyses.

2.3 Water quality parameters

The water quality parameters such as fluoride, phosphate, turbidity, electrical conductivity, and chemical oxygen demand were determined according to methods described by [2]. All the reagents used were analytical grade.

2.3.1 Lead, copper and cadmium

Lead, copper, and cadmium levels in the water samples were determined using the atomic absorption spectrometry method. A 100 ppm stock solution was prepared for Pb, Cu, and Cd. The 0, 1, 2, 3, 4, and

5 ppm, solutions were prepared by serial dilution of the stock solution of the respective metal ion. The wavelengths for the metal ions were Pb; 283.3 nm, Cu; 324.8nm, and Cd; 228.8 nm. Appropriate calibration was done using the standards, and then samples were analyzed for Pb, Cu, and Cd.

2.3.2 Phosphate

Phosphate concentrations in the water samples were analyzed using UV-Vis Spectrophotometer [19] and all the reagents used were of analytical grade. A stock solution of 500 ppm phosphate was prepared by dissolving 2.195 g of potassium dihydrogen phosphate anhydrate in a glass beaker, then transferred into a 1000 mL volumetric flask and filled to the mark with distilled water. From the stock solution, 0, 0.5, 1, 2.5, 5, 7.5, 10, and 12.5 ppm standard solutions of phosphate were prepared.

A 3 M sulphuric acid was prepared in a 500 mL volumetric flask. Ammonium molybdate solution was prepared by dissolving 20 g of ammonium molybdate in about 100 mL distilled water, then transferred into a 500 mL volumetric flask and filled up to the mark with distilled water. A 1.375 g of potassium antimonyl tartrate was dissolved in about 300 mL of distilled water, transferred to a 500 mL volumetric flask. The ascorbic acid solution was prepared by dissolving 1.76 g of ascorbic acid in a 100 mL and diluted to the mark with distilled water.

A mixed solution was prepared by mixing 50 mL of sulphuric acid, 15 mL of ammonium molybdate, 5 mL of potassium antimonyl tatrate, and 30 mL of the ascorbic acid solution that had been made. The mixed solution was stable after 4 hours. To each 50 mL of the standard was added 8 mL of the mixed solution and allowed to stand for 30 minutes for proper colour development. The absorbance readings were taken at 830 nm and used to prepare the calibration curve. The water sample was treated as the standards and was put in a sample cell, then placed in a UV-Vis spectrophotometer for absorbance reading.

2.3.3 Chemical oxygen demand – COD

The COD was determined by redox titration [2], which involved back titration of excess dichromate with ferrous ammonium sulphate solution. Three portions of water samples were prepared in which 50.0 mL of standardized $K_2Cr_2O_7$ was pipetted into a 500 mL Erlenmeyer flask. A 50 ml of 9 M H_2SO_4 was added slowly with stirring. The mixture was cooled to 25°C, and 25.0 mL of the sample was cautiously pipetted into the cooled flask and homogenized. The solution was boiled gently using a hot plate while covered with a watch glass to minimize evaporation. The sample digestion was continued for about one hour and the volume lost to evaporation was replaced with distilled water to keep the solution volume almost constant. The content of the sample flask was cooled to 25°C, 5 drops of ferroin indicator were added and the sample was titrated with 0.15 M ferrous ammonium sulphate until endpoint was reached.

2.3.4 Electrical conductivity – EC

The conductivity was measured using an electrical conductivity meter [20]. The EC meter was turned on and the probe was calibrated using a standard solution. The conductivity meter was calibrated before each sample measurement. The samples were placed in plastic beakers in volumes that

submerged the probe tip. The probe was cleaned with double-distilled water and blot dried before inserting into the sample vessel. The probe tip was in the sample until there was a stable EC reading.

2.3.5 Turbidity

Turbidity of the water sample was measured using an electric turbidity meter [2]. Hexamethylene tetramine reagent was prepared by dissolving 1.0 g of hexamethylene tetramine in distilled water. The hexamethylene tetramine solution was transferred into a 100 mL volumetric flask and filled up to the mark with distilled water. Standard 4000 NTU was prepared by mixing 5 mL of hexamethylene tetramine and 5 mL of hydrazine sulphate in a 100 mL volumetric flask and allowed to stand for 24 hours; the volume was then filled to the mark with distilled water. A 200 NTU was made from the 4000 NTU standard reagent. The 200 NTU solution was added into a sample cell and placed in the turbidity meter. The turbidity meter reading was adjusted to 200 NTU with the aid of a calibration knob. The process was repeated three times until calibration was complete. Water samples were added to the sample cells to the mark and wiped slowly using soft tissue. The sample cell was put in the turbidity meter and a stable reading was taken.

2.3.6 Fluoride

The fluoride concentration in the water samples was analyzed using a fluoride ion-selective electrode [21]. The instrument was calibrated using fluoride standard solutions with concentrations of 0.0, 0.1, 1.0, 3.0, 5.0, 7.0, 10.0, and 20.0 ppm and TISAB II (Total Ionic Strength Adjustment Buffer). The TISAB II was prepared in a 1000mL beaker that contained 500 mL of distilled water, 57 mL glacial acetic acid, 58 g sodium chloride, and 4 g 1, 2-cyclohexylenediaminetetraacetic acid-CDTA. The mixture was stirred to dissolve, and then the beaker was cooled. The pH was adjusted to between 5.0 and 5.5, and the mixture was transferred into a 1000 mL volumetric flask, then filled up to the mark using distilled water.

The fluoride standard solution and TISAB II solution were mixed in the ratio of 1:1. The fluoride measurements for the standards were performed while stirring using magnetic stirrer and magnet stir bar for one minute for all samples. The fluoride concentration readings were taken in millivolt (mV) units and then converted to mg/L using the linear regression of the calibration curve.

2.4 Artificial neural networks

2.4.1 ANN modelling and implementation

The multilayer perceptron feed-forward network, using a backpropagation training algorithm, was adopted with IBM SPSS statistics 20 software. The input data were from experimental results that formed part of this study. The inputs were physico-chemical parameters that included turbidity, COD and EC, and chemical parameters fluoride and phosphate. The output layer had three dependent variables Pb, Cu, and Cd. The re-scaling method for both the input and output layers variables was standardized. The 78 data sets were partitioned into training, testing, and validation in the ratio 3:1:1, respectively.

The artificial neurons trained through supervised learning in which each output neuron was ‘told’ what its desired response to input signals ought to be. The experimental results for Pb, Cu, and Cd were the target outputs from the input signals. Back-propagation was used to adjust the weights of each unit to minimize the error between the target output and the actual output.

Double-layer artificial neural network topologies were used, and the number of neurons in the hidden layers varied from 2 to 6. The activation function for the hidden layer was tangent hyperbolic, while the output was the identity function. The batch network training criteria were adapted, with gradient descent as the optimization algorithm. The network learning rate was 0.4 and momentum 0.9. The network training stopping rules were; 5 steps without a decrease in error, maximum training time 15 minutes, epochs 200, the minimum relative change in training error 0.0001, and minimum change in the training error ratio 0.001. Error function in the ANN model was measured using the sum of squares (SSE) based on the testing samples.

2.4.2 ANN model performance testing

Performance testing was by using sum squared error, Pearson product-moment, and slope-intercept, according to the methods described by [22]. The slope (m) and intercept (b) in the proximity of 1 and 0, respectively, is indicative of better model performance.

2.4.2.1 Sum squared error (SSE)

The summed square of residual represents the sum of the square difference of the predicted values in comparison to the observed values and is given by equation 6.

$$\mathrm{SSE} = \sum_{i=1}^{N} (\mathrm{Sobs} - \mathrm{Scal})^2 \quad (6)$$

Where N is the total number of datasets predicted, S_{obs} is the observed value of the metal cation concentration, and S_{cal} is the calculated (ANN value) value of the metal cation. Lower SSE illustrates better model performance.

2.4.2.2 Pearson product-moment coefficient of correlation, r

The Pearson product-moment coefficient of correlation is given by equation 7.

$$r = \frac{\Sigma(\mathrm{Sobs} - \check{S}obs) \times (Scal - \check{S}cal)}{\sqrt{(\Sigma\ (\mathrm{Sobs} - \check{S}\mathrm{obs})^2 \times\ (\mathrm{Scal} - \check{S}cal)^2)}} \quad (7)$$

Where:
Šcal is the average calculated metal cation concentration. Equation 7 characterizes the strength of the correlation between simulated and observed data. The values of r nearing unity illustrate a good model.

3. Results and Interpretation

3.1 Physico-chemical parameters

The levels of physico-chemical parameters in river Sosiani were as shown in Table 1.

Table 1: Levels of physico-chemical quality parameters

Parameter (Units)	N	Range	Minimum	Maximum	Mean ± Std
EC [µS/cm]	78	1152.0	40.0	1192.0	422.223 ± 363.07
Turbidty [NTU]	78	932.0	4.0	936.0	128.683 ± 208.12
COD [mg/L]	78	2483.0	7.0	2490.0	452.820 ± 689.95

3.2 Chemical parameters

The fluoride had a mean concentration of 0.174 ± 0.155 mg/L, minimum 0.001 mg/L, maximum 0.495 mg/L, and range 0.494 mg; Phosphate levels in the river averaged 76.249 ± 114.772 mg/L, minimum 1.440 mg/L, maximum 438.900 mg/L, and range 437.460 mg/L.

3.3 Observed pollution loads of lead, copper, and cadmium

The pollution loads of Pb, Cu, and Cd from laboratory analysis were as shown in Table 2.

Table 2: Observed pollution loads

Parameter	N	Range	Minimum	Maximum	Mean ± Std dev
Lead [mg/L]	78	1.283	0.137	1.420	0.615 ± 0.293
Copper [mg/L]	78	0.118	0.011	0.129	0.037 ± 0.027
Cadmium [mg/L]	78	0.165	0.040	0.205	0.096 ± 0.030

3.4 Physicochemical and chemical parameters at the sampling sites

The means of physico-chemical and chemical parameters' concentrations at the sampling sites were as shown in Table 3.

Table 3: Physico-chemical and chemical parameter concentrations (mean ± standard deviation)

Site	Fluoride [mg/L]	Phosphate [mg/L]	EC [µS/cm]	Turbidity [NTU]	COD [mg/L]	Pb [mg/L]	Cu [mg/L]	Cd [mg/L]
S1	0.107 ± 0.060	13.98 ± 20.48	41.62 ± 1.21	13.00 ± 8.95	11.20 ± 3.77	0.544 ± 0.325	0.032 ± 0.015	0.082 ± 0.015
S2	0.177 ± 0 .189	8.37 ± 5.64	80.99 ± 25.38	35.40 ± 29.77	26.29 ± 15.64	0.423 ± 0.269	0.027 ± 0.011	0.085 ± 0.022
S3	0.151 ± 0.159	12.64 ± 16.25	109.07 ± 39.20	39.08 ± 39.73	20.56 ± 18.58	0.440 ± 0.205	0.027 ± 0.012	0.091 ± 0.014
S4	0.169 ± 0.168	10.39 ± 7.36	108.55 ± 25.42	49.33 ± 50.97	22.63 ± 23.78	0.409 ± 0.182	0.030 ± 0.017	0.093 ± 0.019
Site	**Fluoride [mg/L]**	**Phosphate [mg/L]**	**EC [µS/cm]**	**Turbidity [NTU]**	**COD [mg/L]**	**Pb [mg/L]**	**Cu [mg/L]**	**Cd [mg/L]**
S5	0.143 ± 0.123	9.57 ± 6.81	143.84 ± 17.96	83.49 ± 119.67	34.00 ± 14.86	0.548 ± 0.276	0.043 ± 0.030	0.096 ± 0.027
S6	0.237 ± 0.212	128.82 ± 140.08	609.84 ± 175.76	224.05 ± 210.63	582.65 ± 311.36	0.784 ± 0.346	0.094 ± 0.035	0.112 ± 0.041

The results from the six sampling points illustrate an increase in pollution from S1 to S6. Upstream, the anthropogenic and industrial pollution is minimal, while the downstream pollution is by industrial and domestic wastewater. For example, site S6 receives wastewater from the nearby informal settlement of Huruma estate. The phosphate level at S1 is the highest and attributed to runoff from the agricultural land.

3. 4 ANN models

The ANN predicted pollution loads of Pb, Cu, and Cd in river Sosiani are in Table 4.

Table 4: ANN pollution loads

Parameter	N	Range	Minimum	Maximum	Mean ± Std dev
ANN-Pb [mg/L]	78	1.282	0.136	1.418	0.614 ±0.293
ANN-Cu [mg/L]	78	0.102	0.009	0.111	0.032 ± 0.023
ANN-Cd [mg/L]	78	0.184	0.011	0.195	0.073 ± 0.033

The double-layer, multilayer perceptron networks gave good performances. Figure 5 shows the ANN architecture with five input variables, five neurons in the first and second hidden layers, respectively, and three output variables, 5-5-5-3 model. Figures 6, 7, and 8 illustrate scatter plots of the actual outputs against the target outputs for lead, copper, and cadmium, respectively. The importance of the independent variables in predicting the dependent variables on a scale of 1.000 were phosphate 0.284, fluoride 0.250, turbidity 0.189, EC 0.151, and COD 0.126.

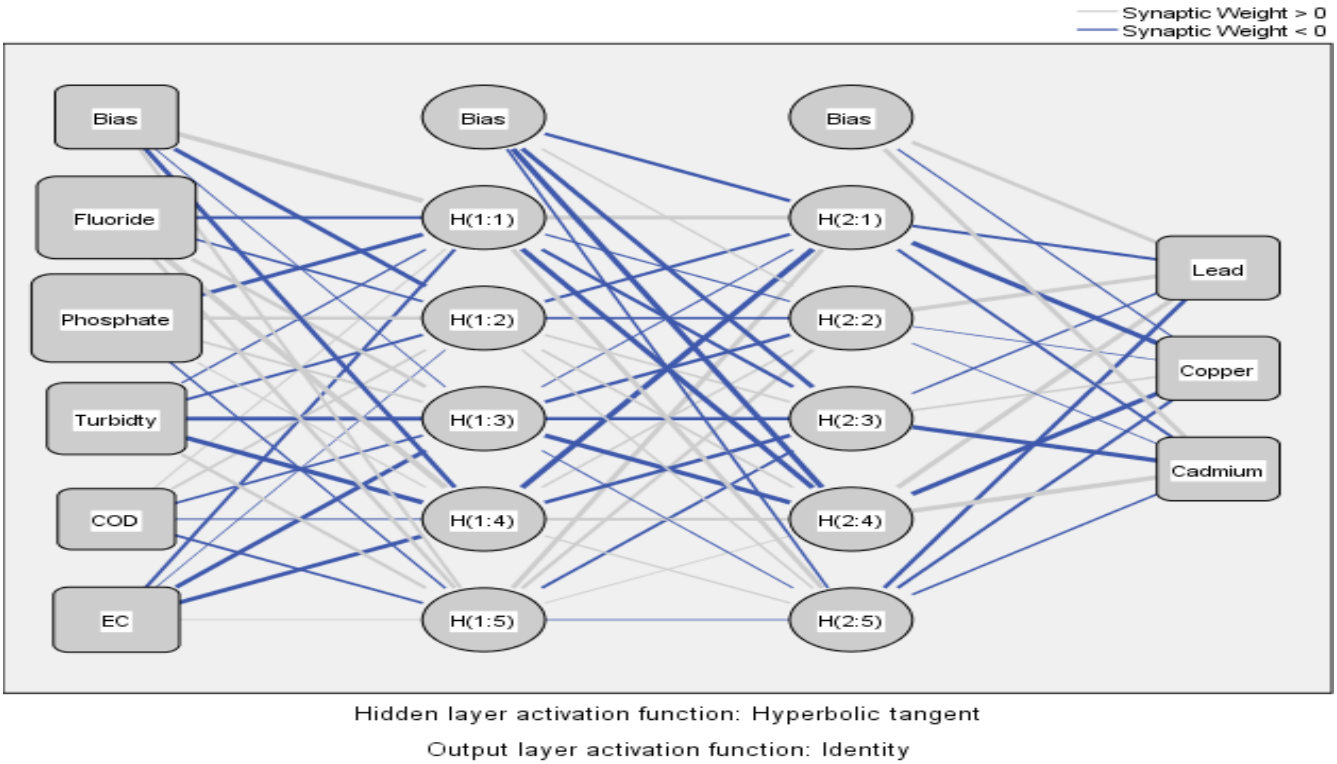

Figure 5: An architecture of artificial neural network of 5-5-5-3 model

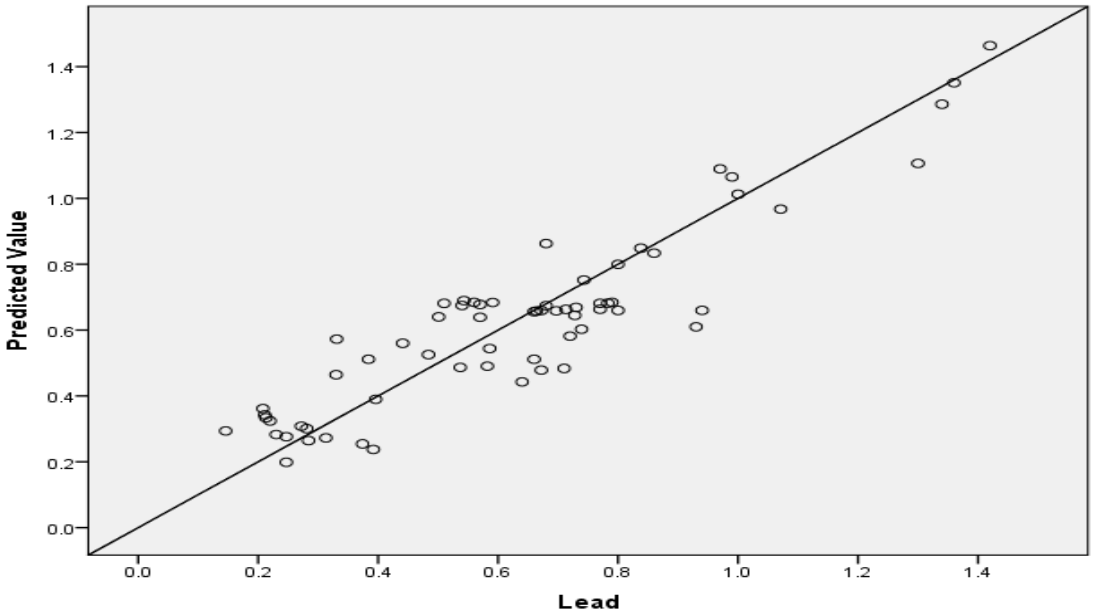

Figure 6: Predicted values against observed values scatter graph for lead

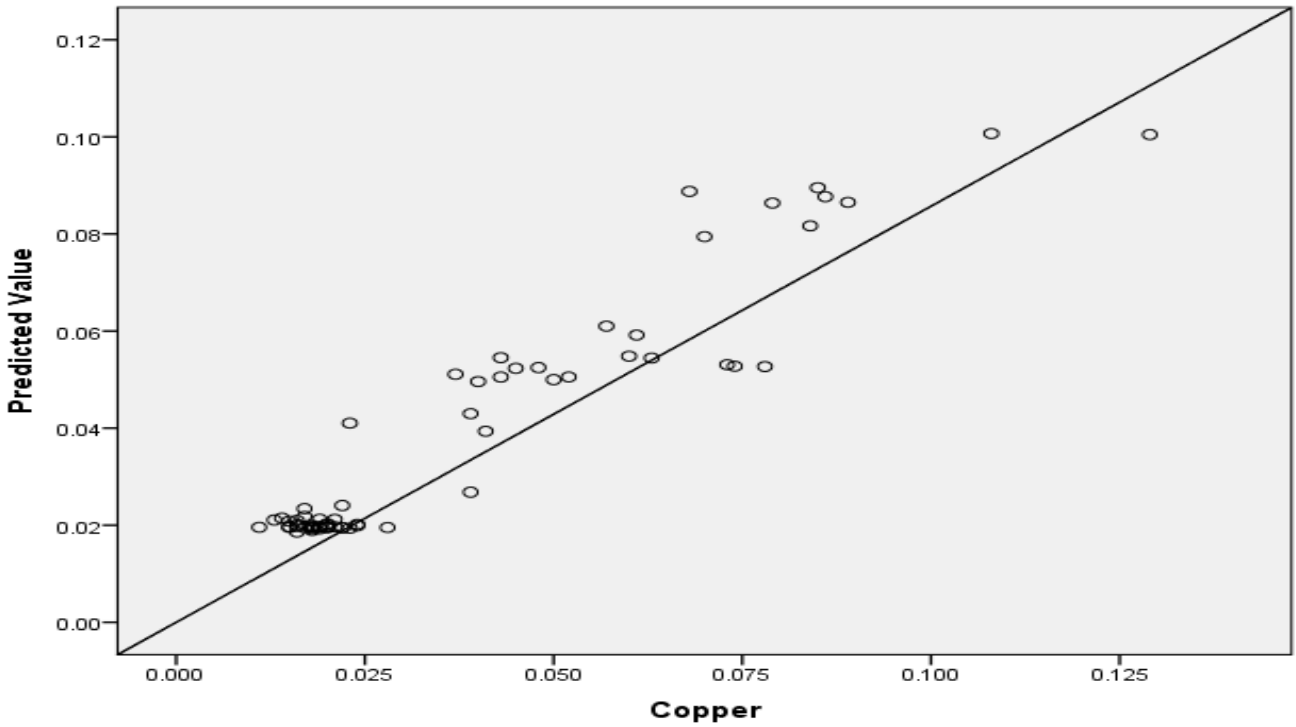

Figure 7: Predicted values against observed values scatter graph for copper

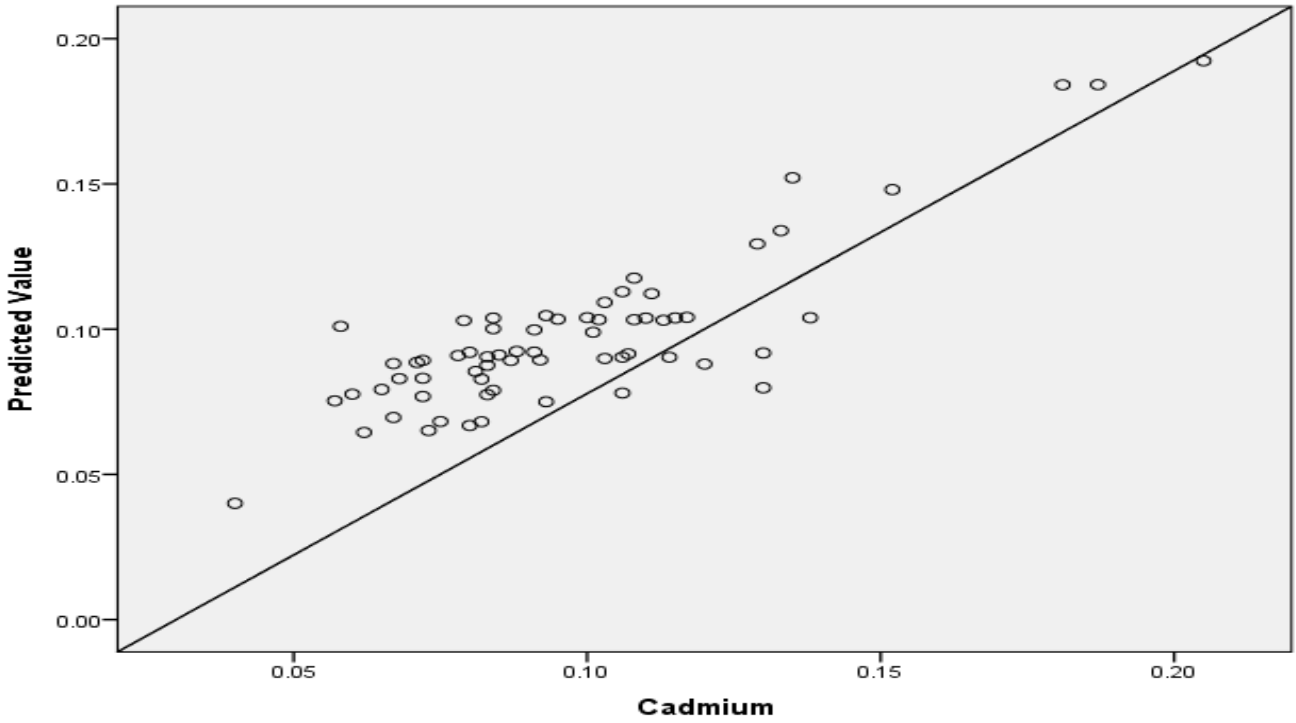

Figure 8: Predicted values against observed values scatter graph for cadmium

3.5 ANN model performances analysis

3.5.1 Sum squared error, SSE

From the sum squared error, the ANN models, 5-5-5-3, and 5-6-6-3 gave the lowest values, and therefore, better performances shown in Table 5.

Table 5: Sum squared error for ANN models

ANN model	Sum squared error		
	Pb	Cu	Cd
5-2-3-3	0.588307	0.014209	0.034052
5-3-4-3	0.733787	0.014209	0.032572
5-4-5-3	0.726887	0.004449	0.017792
5-5-5-3	0.000367	0.004449	0.040112
5-6-6-3	0.000367	0.004449	0.022572

3.5.2 Pearson product-moment correlation coefficient

All the ANN models performed better in predicting the concentrations of Pb, Cu, and Cd from the input data. Table 6 indicates the Pearson product-moment correlation coefficient for lead, copper, and cadmium.

Table 6: Pearson product-moment correlation coefficients for the models

Model	Pearson product-moment correlation coefficient		
	Pb	Cu	Cd
ANN 5-2-3-3	0.9999	0.9882	0.9706
ANN 5-3-4-3	0.9999	0.9882	0.9581
ANN 5-4-5-3	0.9999	0.9910	0.9885
ANN 5-5-5-3	0.9999	0.9910	0.9965
ANN 5-6-6-3	0.9999	0.9910	0.9933

3.5.3 Slope (m) and intercept (b)

The performance model 5-5-5-3 was the best with the slope and intercept, in the proximity of 1 and 0, respectively. Table 7 shows the slopes and intercepts of the ANN model.

Table 7: Slopes and intercepts for ANN model

Model	Predicted parameter	Slope	Intercept
ANN 5-2-3-3	Pb	0.7143	0.200
	Cu	0.7141	0.000
	Cd	0.3501	0.062
ANN 5-3-4-3	Pb	0.6667	0.200
	Cu	0.7143	0.000
	Cd	0.3333	0.060
ANN 5-4-5-3	Pb	0..8000	0.200
	Cu	0.8571	0.000
	Cd	0.6000	0.031
ANN 5-5-5-3	Pb	0.9999	0.000
	Cu	0.8571	0.000
	Cd	1.1111	-0.033
ANN 5-6-6-3	Pb	0.9998	0.000
	Cu	0.8371	0.001
	Cd	0.7831	0.036

4. Discussion

The laboratory results and the ANN predictions (Tables 1, 2 and 3), the levels of EC, copper, and fluoride were below WHO guideline values of 1500 µS/cm, 2 mg/L, and 1.5 mg/L. The lead and cadmium levels exceeded the WHO guideline values of 0.01 mg/L and 0.003 mg/L, respectively. Turbidity exceeded the guideline value of 5 NTU and was likely to affect the acceptability of water from the resource for domestic use [23].

The ability of input variables to predict levels of the outputs in the water resource is due to a correlation explained by the water chemistry. Phosphates work by binding the divalent metals, Pb, Cu, and Cd, to form compounds. For example, soluble Pb can be immobilized by phosphate to form Pb-phosphate species such as pyromorphite, $Pb_5(PO_4)_3Cl$. Agricultural runoffs often include nutrients such as phosphates, and calcinated phosphate is a better adsorbent for Pb^{2+}, Cu^{2+}, and Cd^{2+} [24]. Sources of

fluoride in surface water include weathering of fluoride-bearing mineral rocks and anthropogenic sources such as pharmaceutical products, fertilizers, and toothpaste [25]. Phosphate fertilizers originate from phosphate rocks bearing high levels of fluoride in the form of fluorapatite, $Ca_5(PO_4)_3F$. The fluoride forms complexes with several cations, including Pb^{2+}, Cu^{2+}, and Cd^{2+} [26]. Turbidity is often widely used to detect the occurrence of pollutants in surface water. Metals are particle-bound pollutants in surface water with suspended solids associated with 60 – 97% of total metals in surface water. Turbidity is affected by the properties of the transported sediments, such as shape, size, and mineral composition. Transported suspended solids absorb metals; hence, turbidity is used to detect the occurrence of the metals in surface water [27]. Electrical conductivity is a measure of the ability of water to conduct an electric current and is an indicator of mineral contents and is related to the ionic content of the water sample. It is the ions present in water, such as Pb^{2+}, Cu^{2+}, and Cd^{2+} that carry electrical current, and conductivity increases as the concentration of ions increases. The COD is a measure of the susceptibility to oxidation of the inorganic materials such as Pb, Cu, and Cd, and organic materials present in water bodies. The COD test is non-specific as it does not differentiate between organic and inorganic material present in a water resource [28]. In a related study by [29], the correlation coefficient for ANN models for Pb, Zn, and As were 0.9911, 0.9421, and 0.9637, respectively, and the results related well with the findings of this study.

5. Conclusions

Artificial neural network modeling technique was used to determine the relationships between the concentrations of metal cations, Pb, Zn and As with physico-chemical parameters such as EC, COD, and turbidity as well as the chemical parameters F- and PO3-4 in a water resource. The mean laboratory pollution loads in river Sosiani were 0.615, 0.037, and 0.096 mg/L for Pb, Cu and Cd, while ANN predicted 0.614, 0.032, 0.073 mg /L, respectively. The correlation coefficients for ANN 5-5-5-3 model's predicted and observed values were; Pb 0.9999, Cu 0.9910, and Cd 0.9965. The results from this study show that artificial neural networks can model the behavioral relationship between changes in the water quality variables and the concentrations of Pb, Cu, and Cd. The ANN model was able to learn the nonlinear relationships between the predictor variables in Electral Conductivity, Chemical Oxygen Demand, fluoride, phosphate, and turbidity and target outputs Pd, Cu, and Cd. There is evidence that the proposed ANN model can effectively predict the pollution load in the water resource. However, the study recommends further research with diverse samples to validate these findings.

Acknowledgements

The authors thank the authority of the Department of Chemistry, University of Nairobi, for providing laboratory facilities.

References

[1]. Upma,S., Shikha, S., Rishikesh, K.T., and Ravi, S.P. (2018) Water Pollution due to Discharge of Industrial Effluents with special reference to Uttar Pradesh, India – A review. Int. Arch. App. Sci. Technol **9** (4), 111 – 121.

[2]. Obiewa, J.O., Kariuki, D. K., and Wachira, D. N. (2019) Assimilation of Pollution Loading on Sosiani River in Eldoret Municipality, Kenya: As a Wastewater Management Strategy. American Journal of Water Resources **7** (4), 155-162.

[3]. Tumer, A.E., and Edebali, S. (2015) An Artificial Neural Network Model for Wastewater Treatment Plant of Konya. International Journal of Intelligent Systems Applications in Engineering **3** (4), 131 - 135.

[4]. Guchi , D., and Sukru, D. (2010) Artificial Neural Network Modelling of a Large –Scale Wastewater Treatment Plant Operation. Bioprocess Biosyst Eng **33**, 1051 – 1058.

[5]. Bekkari, N., and Zeddouri, A. (2018) "Using artificial neural network for predicting and controlling the effluent chemical oxygen demand in wastewater treatment plant", Management of Environmental Quality: An International Journal, doi.org/10.1108/MEQ-04-2018-0084.

[6]. Helaluddin, A.B.M., Khalid, R.S., Alaama, M., and Abbas, S.A. (2016) Main Analytical Techniques used for Elemental Analysis in Various Matrices. Tropical Journal of Pharmaceutical Research **15** (2), 427 – 434.

[7]. Bayatzadeh, Z.F., Ghadimi, F. and Fattahi, H. (2017)Use of Artificial Intelligence Techniques to Predict Distribution of Heavy metals in Groundwater of Lakan Lead-Zinc Mine in Iran. Journal of Mining and Environment **8** (1), 35 – 48.

[8]. Alizamir, M. and Sobhanardakani, S. (2017) Predicting Arsenic and Heavy Metals Contamination in Groundwater Resources of Ghaharand Plain Based on Imperialist Competitive Algorithm. Environmental Health Engineering and Management Journal **4** (4), 225 – 231.

[9]. Hicham, E.B., Abdelaziz, A., Imad, M.., and Lancelot, L. (2013) Application of the Artificial Neural Networks of MLP Type for the Prediction of the Levels of Heavy Metals in Moroccan Aquatic Sediments. International Journal of Computational Engineering Research **3** (6), 75 – 81.

[10]. Joyanto,K., Sazal, K., Biplob, K..P., Sajal, S., Aminur, R., and Rafiguel, I. (2018) Charecterization of wastewater from Jhenaidah municipality area, Bangladesh: A combined physico-chemical and statistical approach. AIMS Environmental Science **5**, 389 – 401.

[11]. Mahmoud, S.M., Medhat, A.E.M., Hamdy, A.E., and Seif, G.E.K. (2012) Application of Artificial neural Network (ANN) for the Prediction of EL-AGAMY Wastewater Treatment Plant Performance- EGYPT. Alexandria Engineering Journal **51**, 37 – 43.

[12]. Merenda, M. , Porcar, C., and Iero, D. (2020) Edge Machine Learning for AI-Enabled IoT Devices. Sensors 2020, 10, 2533; doi: 10.3390/s20092533

[13]. Yogeswari, M.K., Dharmalingam, K.., and Mullai, P. (2019) Implementation of Artificial Neural Network Model for Continuous Hydrogen Production Using Confectionery Wastewater. Journal of Environmental Management 252, 1 – 8.

[14]. Zacharis, N.Z. (2016) Predicting Student Academic Performance in Blended Learning Using Artificial Neural Networks. International Journal of Artificial Intelligence and Application 7 (5), 17 – 29.

[15]. Suzana, H. (2009) The Human Brain in Numbers: A linearly scaled-up Primate Brain. Fron Hum Neurosci, doi: 10.3389/neuro. 09.031.2009

[16]. Stafford, R. (2010) Constraints of Biological Neural Networks and Their Consideration in AI Applications. Advances in Artificial Intelligence 2010, 1 - 6

[17]. Tang, J., Yuan, F., Shen, X., Wang, Z., Rao, M., He, Y., Sun, Y., Li, X., Zhang, W., Li, Y., Gao, B., Song, S., Yang, J.J., and Wu, H. (2019) Bridging Biological and Artificial Neural Networks with Emerging Neuromorphic Devices: Fundamentals, Progress, and Challenges. Adv Mater 31, 1 – 33.

[18]. Wang, Y., Li, Y., Song, Y., and Rong, X. (2020) The Influence of the Activation Function in Convolution Neural Network Model of Facial Expression Recognition. Appl. Sci. 2020, 10, 1897; doi: 10.3390/app 10051897

[22]. Aklil, A., Mouflih, M., and Sebti, S. (2004) Removal of Heavy Metal ions from Water by Using Calcined Phosphate as a new Adsorbent. Journal of Hazardous Materials 112 (3), 183 – 190.

[23]. World Health Organization (2017) Guidelines for drinking-water quality, fourth edition incorporating the first addendum.; World Health Organization,. Geneva, Switzerland.

[24]. Kasturya, F., Placitub, S., Bolandc, J., Karnad, R.R., Scheckele, K.G., Smitha, E., Juhasza, A.L. (2019) Relationship between Pb relative bioavailability and bioaccessibility in phosphate amended soil: Uncertainty

associated with predicting Pb immobilization efficacy using in vitro assays. Environment International 131, 1 – 9.

[25]. Ramfeke, L.P., Isahayam, A.C., Ghosh, A., Rambabu, U., Reddy, M.R.P., Popat, K.M., Rebary, B., Kabavat, D., Marathe, K.V., Ghosh, P.K. (2018) Study of Fluoride Content in Some Commercial Phosphate Fertilizers. Journal of Fluorine Chemistry 210, 149 – 155.

[26]. Yao, H.., Zhuang, W., Qian, Y., Xia,B., Yang, Y., Qian, X. (2016) Edtimating and Predicting Metal Concetration Using Online Turbidity Values and water Quality Models in Two Rivers of Taihu Basin, Eastern China. PLoS ONE 11(3): e0152491. doi:10.1371/journal.pone.0152491

[27]. Yao, H., Zhuang, W., Qian, Y., Xia, B., Yang, Y., and Qian, X..(2016) Estimating and Predicting Metal Concentration Using Online Turbidity Values and Water Quality Models in Two Rivers of the Taihu Basin, Eastern China. PLoSONE, 11 (3), 1-15.

[28]. Hattab, N., and Hambli, R. (2014) Prediction of Copper and Chromium Concentrations in Bean Leaves Based on Artificial Neural Network Model. Int.J. Environ. Sci. Technol. 11, 1781 – 1786.

[29]. Alizamir, M. and Sobhanardakani, S. (2016) Forecasting of heavy metals concentration in groundwater resources of Asadabad plain using artificial neural network approach. J.Adv Environ Health Res 4 (2), 68 – 77.

[30].Gholami, R., Kamkar-Rouhani, A., Ardejani, F.D., and Maleki, S. (2011) Prediction of toxic metals concentration using artificial intelligence techniques. Appl Water Sci, 1, 125 – 134.